Kinetic Control and Thermodynamic Selection in the Synthesis of Atomically Precise Gold Nanoclusters

Zhikun Wu,[*,†,‡] Mark A. MacDonald,[§] Jenny Chen,[†] Peng Zhang,[§] and Rongchao Jin[*,†]

[†]Department of Chemistry, Carnegie Mellon University, 4400 Fifth Avenue, Pittsburgh, Pennsylvania 15213, United States

[‡]Key Laboratory of Materials Physics, Anhui Key Laboratory of Nanomaterials and Nanotechnology, Institute of Solid State Physics, Chinese Academy of Sciences (CAS), Hefei 230031, Anhui, China

[§]Department of Chemistry and Institute for Research in Materials, Dalhousie University, Halifax, Nova Scotia, Canada B3H 4J3

Ⓢ *Supporting Information*

ABSTRACT: This work presents a combined approach of kinetic control and thermodynamic selection for the synthesis of monodisperse 19 gold atom nanoclusters protected by thiolate groups. The step of kinetic control allows the formation of a proper size distribution of initial size-mixed $Au_n(SR)_m$ nanoclusters following the reduction of a gold precursor. Unlike the synthesis of $Au_{25}(SR)_{18}$ nanoclusters, which involves rapid reduction of the gold precursor by $NaBH_4$ followed by size focusing, the synthesis of 19-atom nanoclusters requires slow reduction effected by a weaker reducing agent, borane—*tert*-butylamine complex. The initially formed mixture of nanoclusters then undergoes size convergence into a monodisperse product by means of a prolonged aging process. The nanocluster formula was determined to be $Au_{19}(SC_2H_4Ph)_{13}$. This work demonstrates the importance of both kinetic control of the initial size distribution of nanoclusters prior to size focusing and subsequent thermodynamic selection of stable nanoclusters as the final product.

Metal nanoclusters constitute a new class of material that has been intensely pursued in recent years. Nanoclusters comprising ~10 to a few hundred atoms possess properties intermediate between those of the atomic and bulk states. Such properties are caused by the discrete electronic structure of the core due to quantum size effects as well as by the surface of the particle. Among the precious metals, gold nanoclusters have received extensive attention because of their interesting optical properties,[1−4] magnetism,[5,6] fluorescence and electron emissions,[7−15] and redox properties[16−19] as well as their potential applications in fields such as catalysis[20,21] and optics.[22,23] Recently, major advances in the wet chemical synthesis of nanoclusters has been achieved, and it has been possible to control nanoclusters at the atomic level.[24] Some well-defined nanoclusters have been reported.[25] However, only a few can be obtained in bulk quantities and high yields by facile synthetic methods.[26−31] Thus, it is of critical importance to develop synthetic strategies that permit the synthesis of atomically precise nanoclusters for in-depth fundamental studies as well as practical applications. Herein we report a one-pot process for the synthesis of thiolated 19 gold atom nanoclusters that is based on both kinetic control and thermodynamic selection principles.

In a typical synthesis [see the Supporting Information (SI) for details], a solution of a gold salt ($HAuCl_4 \cdot 3H_2O$) was cooled to 0 °C in an ice bath. Phenylethylthiol (denoted as $HS-C_2H_4Ph$) was added to the cold Au(III) solution. The solution was kept under constant stirring (~60 rpm) until the formation of Au(I) aggregates was complete. Next, the solution was vigorously stirred, and then a freshly made toluene solution of borane—*tert*-butylamine complex (5 equiv/mol of Au) was added dropwise over a period of ~8 min. The growth of gold nanoclusters was allowed to proceed for ~60 h. After removal of the precipitates, the solvent was evaporated by rotary evaporation, and the product was thoroughly washed with ethanol. Finally, the nanoclusters were subject to precipitation 2−3 times from a toluene/EtOH solution.

In the synthesis of nanoclusters, the purity of the product is of critical importance. If the product is a mixture, it is very difficult to determine the exact cluster formula and attribute any meaningful properties to the nanoclusters. Therefore, we first characterized the purity of the as-obtained nanoclusters. We used size-exclusion chromatography (SEC) for *preliminary* characterization of the cluster purity. In our previous works, we utilized SEC to isolate $Au_{40}(SR)_{24}$ from $Au_{38}(SR)_{24}$ nanoclusters as well as Pd-doped 25-atom $Pd_1Au_{24}(SR)_{24}$ nanoclusters from homogold $Au_{25}(SR)_{18}$ ones.[32] Thus, SEC may be quite useful as a first check of the product purity. A representative size-exclusion chromatogram of the synthesized nanoclusters is shown in Figure 1. By comparing the online recorded spectra at different retention times of the peak, one finds that all of the spectra are superimposable (Figure 1 inset), indicating the high purity of the nanocluster sample.

The purity of the as-prepared product was also confirmed by subsequent mass spectrometric analysis. We employed electrospray ionization mass spectrometry (ESI-MS) to determine the formula of the nanocluster. ESI is a soft ionization technique and typically does not result in fragmentation of nanoclusters; hence, it is an indispensable tool for nanocluster formula determination.[33−35] For the gold nanoclusters prepared in this work, ESI-MS analysis showed a dominant peak at m/z 5659.3 (Figure 2); it should be noted that CsOAc was added to the nanocluster solution to promote ionization via formation of nanocluster—Cs adducts.[34,35] The low-mass range of the mass spectrum (m/z <5500) consisted of strong signals of $Cs[CsOAc]_n^+$ (peaks 1−13, assigned to n = 16−28, respectively) and some small $Na[CsOAc]_n^+$ signals, as seen in
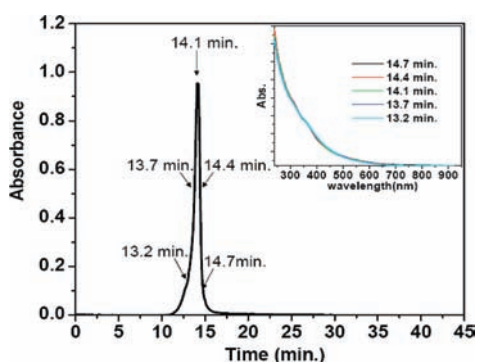
Figure 1. Size-exclusion chromatogram of the nanoclusters [monitored at λ = 330 nm using CH_2Cl_2 (0.5 mL/min) as the eluent]. Inset: online-recorded UV−vis spectra corresponding to different retention times.
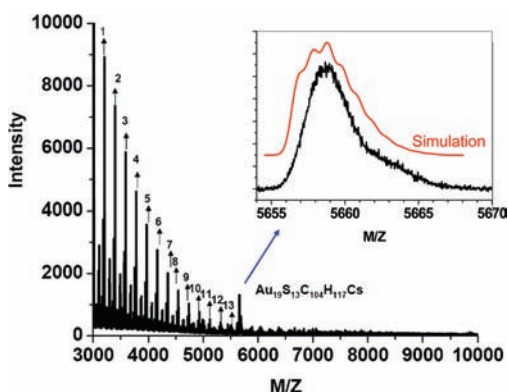

Figure 2. ESI-MS data for $Au_{19}(SC_2H_4Ph)_{13}$ nanoclusters. Inset: isotope pattern of the peak at m/z 5659 (assigned to the nanocluster−Cs^+ adduct) and a simulated pattern for $[Au_{19}(SC_8H_9)_{13}Cs]^+$ with a resolving power of 5000. Peaks 1−13 correspond to $(CsOAc)_nCs^+$ (n = 16−28).

previous work.[35] The nanocluster signal at m/z 5659.3 was quite clean; no other nanoclusters were found in the mass spectrum up to m/z 10 000. The isotope pattern was not resolved because of the relatively weak signal of the cluster−Cs^+ adduct, but the peak width was consistent with the simulation (Figure 2, inset). Hence, the charge state was 1+ (positive mode). The mass of the nanocluster−Cs^+ adduct was thus determined to be 5659.3 Da. On the basis of the exact mass, the formula was readily deduced to be Au_{19}-$(SC_2H_4Ph)_{13}Cs^+$ (theoretical mass: 5658.8 Da). Laser desorption ionization mass spectrometry (LDI-MS) analysis showed a core with a mass of 3−4 kDa, consistent with the formula. This formula was also supported by other analyses, including X-ray photoelectron spectroscopy (XPS) and thermogravimetric analysis (TGA) (see below).

A potential concern is whether the nanocluster bears any counterions, as in the case of $Au_{25}(SC_2H_4Ph)_{18}[N(C_8H_{17})_4]$.[1,26] NMR analysis (Figure S1 in the SI) ruled out the presence of $[N(C_8H_{17})_4]^+$ (abbreviated TOA^+), although TOABr was used in our synthesis. Moreover, salt tests involving addition of silver trifluoroacetate to the nanocluster solution (in THF solvent; see the SI for experimental details) did not result in any precipitate, indicating the absence of Br^- (or Cl^-) as the counterion of the nanocluster. XPS analysis of the product also did not find halides in the nanocluster (Figure 3a). Elemental quantification by XPS gave an Au/S ratio of 1.43 ± 0.04 (for details, see the SI), consistent with the expected value (19/13 = 1.46). The high-
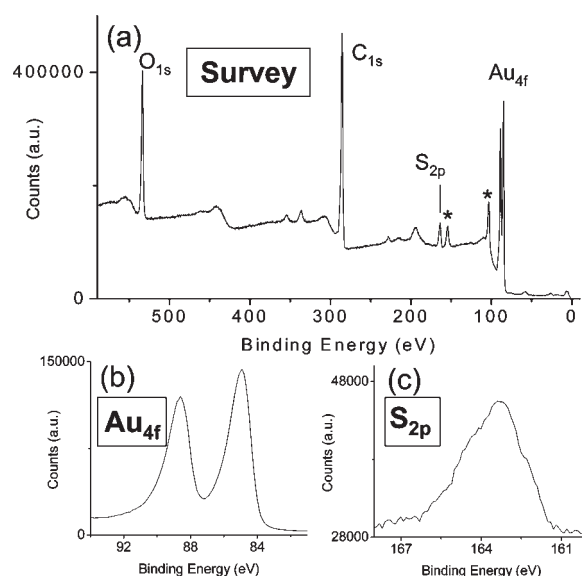

Figure 3. XPS analysis of the Au_{19} nanocluster: (a) survey scan; (b) Au_{4f} (c) S_{2p}. The peaks marked with * in (a) are from the Si substrate.

resolution Au_{4f} and S_{2p} spectra are shown in Figure 3b,c. The $Au_{4f_{7/2}}$ peak is located at 84.9 eV and the S_{2p} peak at 163.4 eV. Relative to the XPS data for Au_{25},[31b] the Au_{19} sample showed a ∼0.5 eV shift toward higher binding energy. The positive shift of the binding energy for Au_{19} relative to Au_{25} suggests a larger band gap for Au_{19}. On the basis of the above NMR, salt test, and XPS analyses, the Au_{19} nanocluster should be charge-neutral. The neutral state is indeed quite common in nanoclusters reported to date [except the case of $Au_{25}(SR)_{18}^-$]. Taken together, the data determined the nanocluster formula to be $[Au_{19}(SC_2H_4Ph)_{13}]^0$. TGA further confirmed this conclusion. A weight loss of 31.6% was observed (Figure S2), which agrees with the expected value (32.2 wt %).

With respect to the growth mechanism of $Au_{19}(SC_2H_4Ph)_{13}$ nanoclusters, we found that during the reaction process (e.g., aging for 38 h) a small amount of $Au_{25}(SC_2H_4Ph)_{18}$ (yield <0.5%) was indeed formed, and it could be separated by CH_3CN extraction of the crude product (see Figure S3). Notably, when the reducing agent (borane−*tert*-butylamine complex) was changed to $NaBH_4$, the dominant product indeed became Au_{25}. Thus, the reducing reagent plays a critical role in controlling the final nanocluster size. Borane−*tert*-butylamine complex is a much weaker reducing agent than $NaBH_4$. During the reaction process, we observed that upon addition of borane−*tert*-butylamine complex, the gold precursor solution slowly changed from yellow to orange and then to black over a ∼15 min period, whereas with $NaBH_4$, the solution color immediately changed to black within a few seconds. These results indicate that the rate of reduction of Au(I) to Au(0) greatly influences the nanocluster size, that is, it is a kinetically controlled process. The critical importance of the reduction step and subsequent nucleation process is also reflected in our previous works. One example is the synthesis of Au_{24}-$(SC_2H_4Ph)_{20}$ clusters,[35b] where decreasing the amount of reducing agent ($NaBH_4$) from 10 to 1 equiv/mol of Au and adding the reducing agent in a dropwise manner to slow the production of the Au(0) species afforded $Au_{24}(SC_2H_4Ph)_{20}$ rather than $Au_{25}(SC_2H_4Ph)_{18}$. Another example is the synthesis of Ag_7 using ethanol as the solvent instead of water, where decreasing the amount of reducing reagent resulted in the
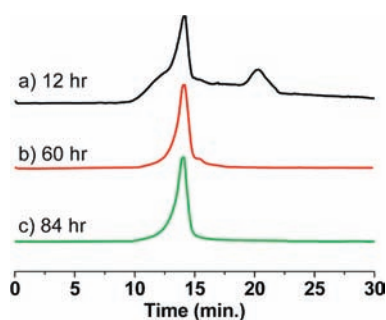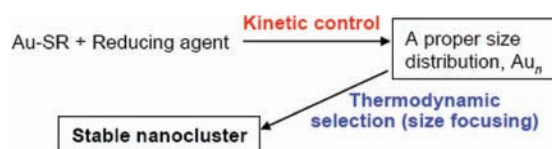
Figure 4. Size evolution of the product as monitored by SEC (absorbance at 330 nm vs aging time).

Scheme 1. Kinetic Control and Thermodynamic Selection in the Synthesis of Atomically Monodisperse Nanoclusters

Figure 5. PXRD patterns of $Au_{19}(SR)_{13}$ and $Au_{25}(SR)_{18}$ nanoclusters (Cu Kα source).

formation of Ag_7.[36] In these cases, the syntheses essentially involve kinetic control. The nucleation mechanism remains a major challenge, and the Au(I) intermediate also deserves further exploration for nanocluster synthesis.[37,38]

Apart from the importance of kinetic control in nanocluster synthesis, another important factor is the thermodynamic stability of nanoclusters. Both principles were indeed critical in the successful synthesis of $Au_{19}(SC_2H_4Ph)_{13}$ nanoclusters. Stable nanoclusters can exist in solution after aging for a long time, while unstable nanoclusters are converted either to stable ones or to Au(I)−SR.[24] As in the case of Au_{25} synthesis,[28] Au(I)−SR species were observed in the final product, as evidenced by TGA analysis of the residue of the reaction product after toluene/EtOH extractions (see Figure S4). In the synthesis of $Au_{19}(SR)_{13}$, an interesting size-focusing process was observed. We used SEC to monitor the size evolution of the crude product with time (Figure 4). The initial product contained a range of nanocluster sizes that included Au_{19} (retention time ≈ 14.1 min) (Figure 4, profile a). After ∼60 h of aging, most species other than Au_{19} disappeared, and Au_{19} became the predominant species (Figure 4, profile b); further aging did not produce appreciable changes; thus, we stopped the reaction after ∼60 h of aging. This experiment demonstrated that the size-focusing process occurring in the aging step is critical for improving the product purity, and thermodynamic selection was apparently in operation in the synthesis of high-purity Au_{19} nanoclusters. Interestingly, recent work by Pettibone and Hudgens[4] identified a size-selective synthetic pathway for small gold clusters capped by phosphine that bears some resemblance to the size-focusing process in the gold−thiolate system.

Overall, the synthesis of monodisperse $Au_{19}(SR)_{13}$ nanoclusters demonstrates two major factors: (i) kinetic control of the initial size distribution and (ii) thermodynamic selection (or size focusing) during the aging process to give a final cluster species that is relatively robust in the size distribution (Scheme 1). Control of the initial size distribution is very important, as a size distribution that is too broad would lead to two or multiple stable nanoclusters in the final product after size focusing. The
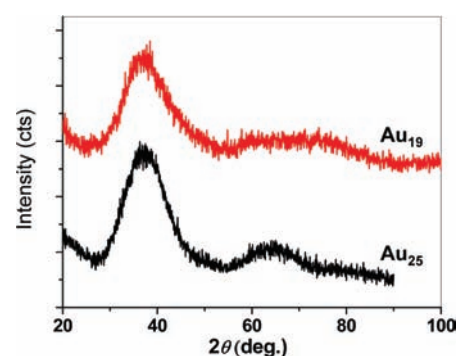
thermodynamic basis of the size-focusing process is apparently the stability property of specific-sized $Au_n(SR)_m$ nanoclusters, raising the question of what determines the particular stability of magic-sized nanoclusters. This constitutes the most intriguing question in the field, and it remains to be addressed in future research. The size-focusing mechanism has been identified to be ubiquitous in the synthesis of many thiolated nanoclusters, such as $Au_{20}(SR)_{16}$, $Au_{24}(SR)_{20}$, $Au_{25}(SR)_{18}$, $Au_{38}(SR)_{24}$, and Au_{144}-$(SR)_{60}$. In this sense, all of the nanoclusters that are made by size focusing are more or less thermodynamically stable (as opposed to kinetically stable). However, it is difficult to have a precise ruler of kinetic versus thermodynamic stability as a function of size. The overall stability of Au_{19} is somewhat less than that of Au_{25}. This may explain the fact that Au_{25} is ubiquitously observed in many syntheses whereas Au_{19} needs more specific conditions for its formation. It remains to be seen whether the principles of kinetic control and thermodynamic selection can be extended to other types of nanoclusters.[39]

The $Au_{19}(SC_2H_4Ph)_{13}$ nanoclusters showed much less prominent absorption peaks than $Au_{25}(SC_2H_4Ph)_{18}$ and Au_{38}-$(C_2H_4Ph)_{24}$ (Figure S5), and only two weak peaks were found at 310 and 365 nm; this is presumably linked to its structure. Attempts to crystallize this nanocluster were not successful. Nevertheless, the structural aspect of $Au_{19}(SC_2H_4Ph)_{13}$ nanoclusters is worthy of a brief discussion. Previous works[40] have reported a D_{5h} geometry for $[Pt_{19}(CO)_{22}]^{4-}$ and an interpenetrated biicosahedral structure for both $Au_{12}Ag_7(PMe_2Ph)_{10}$-$(NO_3)_9$ and $Au_{17}Ag_2(PMe_2Ph)_{10}(NO_3)_9$. Recently, Femoni et al.[41] reported an interpenetrated biicosahedral $[Pt_{19}(CO)_{17}]^{8-}$ core. The powder X-ray diffraction (PXRD) pattern of the $Au_{19}(SR)_{13}$ nanoclusters showed a strong peak at ∼37° and a very broad feature at 55−85°; the latter is quite different from what appears in the PXRD pattern of icosahedral $Au_{25}(SR)_{18}$ nanoclusters (Figure 5). Thus, $Au_{19}(SC_2H_4Ph)_{13}$ perhaps does not adopt an icosahedron-based structure.

In summary, we have developed a size-focusing method for the synthesis of a new cluster species identified to be 19 gold atom nanoclusters. A key to the synthesis is control of the reduction step: by replacing $NaBH_4$ (a strong reducing agent) with a weaker one (borane−*tert*-butylamine complex), the reaction rate of the production of Au(0) was significantly decreased, leading to a suitable size distribution that eventually underwent size convergence into a monodisperse Au_{19} nanocluster after spontaneous size focusing. The nanocluster composition was determined to be $[Au_{19}(SC_2H_4Ph)_{13}]^0$. This work demonstrates the importance of both kinetic control and thermodynamic selection in the synthesis

9672

dx.doi.org/10.1021/ja2028102 |*J. Am. Chem. Soc.* 2011, 133, 9670–9673

of monodisperse nanoclusters. It is hoped that the present work will provide some guidance for the future synthesis of a full series of atomically precise nanoclusters for fundamental science studies and practical applications.

■ ASSOCIATED CONTENT

ⓢ Supporting Information. Experimental details of the synthesis and characterization of the material (Supporting Figures S1–S5). This material is available free of charge via the Internet at http://pubs.acs.org.

■ AUTHOR INFORMATION

Corresponding Author
zkwu@issp.ac.cn; rongchao@andrew.cmu.edu

■ ACKNOWLEDGMENT

■ REFERENCES

(1) Zhu, M.; Aikens, C. M.; Hollander, F. J.; Schatz, G. C.; Jin, R. *J. Am. Chem. Soc.* **2008**, *130*, 5883.

(2) Wyrwas, R. B.; Alvarez, M. M.; Khoury, J. T.; Price, R. C.; Schaaff, T. G.; Whetten, R. L. *Eur. Phys. J. D* **2007**, *43*, 91.

(3) Shichibu, Y.; Negishi, Y.; Watanabe, T.; Chaki, N. K.; Kawaguchi, H.; Tsukuda, T. *J. Phys. Chem. C* **2007**, *111*, 7845.

(4) (a) Pettibone, J. M.; Hudgens, J. W. *ACS Nano* **2011**, *5*, 2989. (b) Pettibone, J. M.; Hudgens, J. W. *J. Phys. Chem. Lett.* **2010**, *1*, 2536.

(5) Zhu, M.; Aikens, C. M.; Hendrich, M. P.; Gupta, R.; Qian, H.; Schatz, G. C.; Jin, R. *J. Am. Chem. Soc.* **2009**, *131*, 2490.

(6) Negishi, Y.; Tsunoyama, H.; Suzuki, M.; Kawamura, N.; Matsushita, M. M.; Maruyama, K.; Sugawara, T.; Yokoyama, T.; Tsukuda, T. *J. Am. Chem. Soc.* **2006**, *128*, 12034.

(7) Wang, G.; Huang, T.; Murray, R. W.; Menard, L.; Nuzzo, R. G. *J. Am. Chem. Soc.* **2005**, *127*, 812.

(8) Shibu, E. S.; Pradeep, T. *Chem. Mater.* **2011**, *23*, 989.

(9) Bigioni, T. P.; Whetten, R. L.; Dag, Ö. *J. Phys. Chem. B* **2000**, *104*, 6983.

(10) Sakamoto, M; Tachikawa, T.; Fujitsuka, M.; Majima, T. *J. Am. Chem. Soc.* **2009**, *131*, 6.

(11) (a) Zhou, C.; Sun, C.; Yu, M.; Qin, Y.; Wang, J.; Kim, M.; Zheng, J. *J. Phys. Chem. C* **2010**, *114*, 7727. (b) Bao, Y.; Zhong, C.; Vu, D. M.; Temirov, J. P.; Dyer, R. B.; Martinez, J. S. *J. Phys. Chem. C* **2007**, *111*, 12194.

(12) Wu, S.; Zeng, H.; Schelly, Z. A. *J. Phys. Chem. B* **2005**, *109*, 18715.

(13) Huang, X.; Zhou, X.; Wu, S.; Wei, Y.; Qi, X.; Zhang, J.; Boey, F.; Zhang, H. *Small* **2010**, *6*, 513.

(14) Devadas, M. S.; Kim, J.; Sinn, E.; Lee, D.; Goodson, T., III; Ramakrishna, G. *J. Phys. Chem. C* **2010**, *114*, 22417.

(15) Hamouda, R.; Bellina, B.; Bertorelle, F.; Compagnon, I.; Antoine, R.; Broyer, M.; Rayane, D.; Dugourd, P. *J. Phys. Chem. Lett.* **2010**, *1*, 3189.

(16) (a) Ingram, R. S.; Hostetler, M. J.; Murray, R. W.; Schaaff, T. G.; Khoury, J. T.; Whetten, R. L.; Bigioni, T. P.; Guthrie, D. K.; First, P. N. *J. Am. Chem. Soc.* **1997**, *119*, 9279. (b) Georganopoulou, D. G.; Mirkin, M. V.; Murray, R. W. *Nano Lett.* **2004**, *4*, 1763.

(17) Zhu, M.; Chan, G.; Qian, H.; Jin, R. *Nanoscale* **2010**, *3*, 1703.

(18) (a) Yang, Y.; Chen, S. *Nano Lett.* **2003**, *3*, 75. (b) Chen, W.; Chen, S. W. *Angew. Chem., Int. Ed.* **2009**, *48*, 4386.

(19) (a) Quinn, B. M.; Liljeroth, P.; Ruiz, V.; Laaksonen, T.; Kontturi, K. *J. Am. Chem. Soc.* **2003**, *125*, 6644. (b) Antonello, S.; Holm, A. H.; Instuli, E.; Maran, F. *J. Am. Chem. Soc.* **2007**, *129*, 9836. (c) Garca-Raya, D.; Madueo, R.; Blzquez, M.; Pineda, T. *J. Phys. Chem. C* **2009**, *113*, 8756.

(20) (a) Zhu, Y.; Qian, H.; Drake, B. A.; Jin, R. *Angew. Chem., Int. Ed.* **2010**, *49*, 1295. (b) Zhu, Y.; Qian, H.; Zhu, M.; Jin, R. *Adv. Mater.* **2010**, *22*, 1915. (c) Zhu, Y.; Wu, Z.; Gayathri, G. C.; Qian, H.; Gil, R. R.; Jin, R. *J. Catal.* **2010**, *271*, 155.

(21) (a) Liu, Y.; Tsunoyama, H.; Akita, T.; Tsukuda, T. *Chem. Commun.* **2010**, *46*, 550. (b) Liu, Y.; Tsunoyama, H.; Akita, T.; Xie, S.; Tsukuda, T. *ACS Catal.* **2011**, *1*, 2.

(22) Ramakrishna, G.; Varnavski, O.; Kim, J.; Lee, D.; Goodson, T. *J. Am. Chem. Soc.* **2008**, *130*, 5032.

(23) Muhammed, M. A. H.; Shaw, A. K.; Pal, S. K.; Pradeep, T. *J. Phys. Chem. C* **2008**, *112*, 14324.

(24) Jin, R.; Qian, H.; Wu, Z.; Zhu, Y.; Zhu, M.; Mohanty, A.; Garg, N. *J. Phys. Chem. Lett.* **2010**, *1*, 2903.

(25) Jin, R. *Nanoscale* **2010**, *2*, 343 and references therein.

(26) (a) Donkers, R. L.; Lee, D.; Murray, R. W. *Langmuir* **2004**, *20*, 1945. (b) Angel, L. A.; Majors, L. T.; Dharmaratne, A. C.; Dass, A. *ACS Nano* **2010**, *4*, 4691.

(27) Shichibu, Y.; Negishi, Y.; Tsukuda, T.; Teranishi, T. *J. Am. Chem. Soc.* **2005**, *127*, 13464.

(28) (a) Zhu, M.; Lanni, E.; Garg, N.; Bier, M. E.; Jin, R. *J. Am. Chem. Soc.* **2008**, *130*, 1138. (b) Wu, Z.; Suhan, J.; Jin, R. *J. Mater. Chem.* **2009**, *19*, 622.

(29) (a) Qian, H.; Zhu, Y.; Jin, R. *ACS Nano* **2009**, *3*, 3795. (b) Qian, H.; Eckenhoff, W. T.; Zhu, Y.; Pintauer, T.; Jin, R. *J. Am. Chem. Soc.* **2010**, *132*, 8280. (c) MacDonald, M.; Zhang, P.; Chen, N.; Qian, H.; Jin, R. *J. Phys. Chem. C* **2011**, *115*, 65. (d) Knoppe, S.; Dharmaratne, A. C.; Schreiner, E.; Dass, A.; Burgi, T. *J. Am. Chem. Soc.* **2010**, *132*, 16783.

(30) Levi-Kalisman, Y.; Jadzinsky, P. D.; Kalisman, N.; Tsunoyama, H.; Tsukuda, T.; Bushnell, D. A.; Kornberg, R. D. *J. Am. Chem. Soc.* **2011**, *133*, 2976.

(31) (a) Qian, H.; Jin, R. *Nano Lett.* **2009**, *9*, 4083. (b) MacDonald, M. A.; Zhang, P.; Qian, H.; Jin, R. *J. Phys. Chem. Lett.* **2010**, *1*, 1821.

(32) (a) Qian, H.; Zhu, Y.; Jin, R. *J. Am. Chem. Soc.* **2010**, *132*, 4583. (b) Qian, H.; Barry, E.; Zhu, Y.; Jin, R. *Acta Phys. Chim. Sin.* **2011**, *27*, 513.

(33) (a) Negishi, Y.; Nobusada, K.; Tsukuda, T. *J. Am. Chem. Soc.* **2005**, *127*, 5261. (b) Chaki, N. K.; Negishi, Y.; Tsunoyama, H.; Shichibu, Y.; Tsukuda, T. *J. Am. Chem. Soc.* **2008**, *130*, 8608.

(34) Fields-Zinna, C. A.; Sampson, J. S.; Crowe, M. C.; Tracy, J. B.; Parker, J. F.; deNey, A. M.; Muddiman, D. C.; Murray, R. W. *J. Am. Chem. Soc.* **2009**, *131*, 13844.

(35) (a) Zhu, M.; Qian, H.; Jin, R. *J. Am. Chem. Soc.* **2009**, *131*, 7220. (b) Zhu, M.; Qian, H.; Jin, R. *J. Phys. Chem. Lett.* **2010**, *1*, 1003.

(36) (a) Wu, Z.; Lanni, E.; Chen, W.; Bier, M.; Ly, D. R.; Jin, R. *J. Am. Chem. Soc.* **2009**, *131*, 6535. (b) Wu, Z.; Jiang, D.; Lanni, E.; Bier, M.; Jin, R. *J. Phys. Chem. Lett.* **2010**, *1*, 1423.

(37) (a) Goulet, P. J. G.; Lennox, R. B. *J. Am. Chem. Soc.* **2010**, *132*, 9582. (b) Li, Y.; Zaluzhna, O.; Xu, B.; Gao, Y.; Modest, J. M.; Tong, Y. J. *J. Am. Chem. Soc.* **2011**, *133*, 2092.

(38) Hussain, I.; Graham, S.; Wang, Z.; Tan, B.; Sherrington, D. C.; Rannard, S. P.; Cooper, A. I.; Brust, M. *J. Am. Chem. Soc.* **2005**, *127*, 16398.

(39) Cathcart, N.; Kitaev, V. *J. Phys. Chem. C* **2010**, *114*, 16010. (b) Finney, E. E.; Finke, R. G. *Chem. Mater.* **2009**, *21*, 4468.

(40) (a) Washecheck, D. M.; Wucherer, E. J.; Dahl, L. F.; Ceriotti, A.; Longoni, G.; Manassero, M.; Sansoni, M.; Chini, P. *J. Am. Chem. Soc.* **1979**, *101*, 6110. (b) Nunokawa, K.; Ito, M.; Sunahara, T.; Onaja, S.; Ozeki, T.; Chiba, H.; Funahashi, Y.; Masuda, H.; Yonezawa, T.; Nishihara, H.; Nakamoto, M.; Yamamoto, M. *Dalton Trans.* **2005**, 2726.

(41) Femoni, C.; Iapalucci, M. C.; Longoni, G.; Zacchini, S.; Zarra, S. *J. Am. Chem. Soc.* **2011**, *133*, 2406.